Organic−Inorganic Hybrid Materials Incorporating Phosphorus-Containing Dendrimers

Cédric-Olivier Turrin,[†] Valérie Maraval,[†] Anne-Marie Caminade,*[,†,§] Jean-Pierre Majoral,*[,†,||] Ahmad Mehdi,[‡] and Catherine Reyé*[,‡,⊥]

Laboratoire de Chimie de Coordination du CNRS, 205, Route de Narbonne, 31077 Toulouse Cedex 4, France, and Laboratoire de chimie moléculaire et organisation du solide, UMR 5637, Université Montpellier-II, case 007 34095 Montpellier Cedex 5, France

Received June 20, 2000. Revised Manuscript Received October 18, 2000

Phosphorus-containing dendrimers of first, second, and third generation with various peripheral functional groups and bearing a hydrolyzable $Si(OEt)_3$ group at the core have been prepared. Two synthetic routes were used: either the $Si(OEt)_3$ group was introduced from the start by reaction of $(EtO)_3Si(CH_2)_3PPh_2$ with an azide according to the Staudinger reaction (**A** series of dendrimers) or the $Si(OEt)_3$ group was grafted to the core in the last step by reaction of 3-aminopropyltriethoxysilane with a vinyl group at the core (**B** series of dendrimers). The silylated dendrimers were characterized by elemental analyses and ^1H, ^{13}C, ^{31}P, and ^{29}Si NMR spectroscopies. The cohydrolysis and polycondensation of these macromolecules with a defined and varying number of equivalents of tetraethoxysilane (TEOS) was carried out via sol−gel protocol, giving rise to dendrimer−silica xerogels. It was proven by ^{31}P NMR spectroscopy that the dendrimers were not damaged during the sol−gel process, and it was shown by ^{29}Si NMR spectroscopy that the dendrimer was covalently linked to the silica matrix by one Si−C bond. The texture of materials was determined by BET measurements. It was shown from elemental and thermogravimetric analysis that the percentage of incorporated organic part was notable but always inferior to the theoretical value.

Introduction

Dendrimers, which are highly branched regular three-dimensional monodisperse macromolecules with a tree-like structure, have recently raised considerable attention.[1,2] Indeed, they offer a wide range of unusual physical and chemical properties mainly due to the presence of a defined number of peripheral functional groups as well as internal cavities (guest−host systems), the core bearing or not a functional group.[3,4] They have already found numerous applications[5] including metal complexation[5d] and also use as catalysts.[6] With the view of possible applications such as supported catalysts,[7] chromatographic supports,[7−10] or porous menbranes,[10] for example, immobilization of dendrimers on a solid support is of interest. In a continuation of our research on phosphorus-containing dendrimers,[2,11] we decided to prepare hybrid materials in which the dendrimer should be covalently bound to a silica matrix by a Si−C bond. Indeed, immobilization of dendrimers on silica has been previously reported by grafting dendrimers[12] or dendrons[13] on the surface of silica gels or by constructing

* To whom correspondence should be addressed.
[†] CNRS.
[‡] Université Montpellier-II.
[§] Fax: 33 5 61 55 30 03. E-mail: caminade@lcc-toulouse.fr.
[||] Fax: 33 5 61 55 30 03. E-mail: majoral@lcc-toulouse.fr.
[⊥] Fax: 33 4 67 14 38 52. E-mail: reye@crit.univ-montp2.fr.

(1) Reviews: Tomalia, D. A.; Naylor, A.; Goddard, W. A., III. *Angew. Chem., Int. Ed. Engl.* **1990**, *29*, 138. Mekelburger, H. B.; Jaworek, W.; Vögtle, F. *Angew. Chem., Int. Ed. Engl.* **1992**, *31*, 1571. Newkome, G. R.; Moorefield, C. N.; Vögtle, F. *Dendritic Molecules, Concepts, Synthesis, Perspectives*; VCH: Weinheim, 1996. Gorman, C. *Adv. Mater.* **1998**, *10*, 295. Chow, H. F.; Mong, T. K. K.; Nongrum, M. F.; Wan, C. W. *Tetrahedron* **1998**, *54*, 8543. Fischer, M.; Vögtle, F. *Angew. Chem., Int. Ed.* **1999**, *38*, 884. Bosman, A. W.; Janssen, H. M.; Meijer, E. W. *Chem. Rev.* **1999**, *99*, 1665.

(2) Majoral, J.-P.; Caminade, A.-M. *Chem. Rev.* **1999**, *99*, 845.

(3) Tomalia, D. A.; Durst, H. D. In *Topics in Current Chemistry, Vol. 165; Supramolecular Chemistry 1: Directed Synthesis and Molecular Recognition*; Weber, E., Ed.; Springer-Verlag: Berlin, 1993; pp 193−313.

(4) Gitsov, I.; Wooley, K. L.; Hawker, J.; Ivanova, P. T.; Fréchet, J. M. J. *Macromolecules* **1993**, *26*, 5621. Jansen, J. F. G. A.; de Brabander-van den Berg, E. M. M.; Meijer, E. W. *Science* **1994**, *266*, 1226. Knapen, J. W. J.; van der Made, A. W.; de Wilde, J. C.; van Leeuwen, P. W. N. M.; Wijkens, P.; Grove, D. M.; van Koten, G. *Nature* **1994**, *372*, 659.

(5) (a) Mattews, O. A.; Shipway, A. N.; Stoddart, J. F. *Prog. Polym. Sci.* **1998**, *23*, 1. (b) Frechet, J. M. J.; Hawker, C. J.; Gitsov, I.; Leon, J. W. *Pure Appl. Chem.* **1996**, *10*, 1399. (c) Ardin, N.; Astruc, D. *Bull. Soc. Chim. Fr.* **1995**, *132*, 875. (d) Caminade, A.-M; Laurent, R.; Chaudret, B.; Majoral, J.-P. *Coord. Chem. Rev.* **1998**, *178−180*, 793. (e) Bianchini, C.; Burnaby, D. J.; Evans, J.; Fredani, P.; Meli, A.; Oberhauser, W.; Psaro, R.; Sordelli, L.; Vizza, F. *J. Am. Chem. Soc.* **1999**, *121*, 5961.

(6) Knapen, J. W. J.; van der Made, A. W.; de Wilde, J. C.; van Leeuwen, P. W. N. M.; Wijkens, P.; Grove, D. M.; van Koten, G. *Nature* **1994**, *372*, 659. Reetz, M. T.; Lohmer, G.; Schwickardi, R. *Angew. Chem., Int. Ed. Engl.* **1997**, *36*, 1526. Reetz, M. T. *Top. Catal.* **1997**, *4*, 187. Maraval, V.; Laurent, R.; Caminade, A.-M.; Majoral, J.-P. *Organometallics* **2000**, *19*, 4025.

(7) Ko, E. I. *CHEMTECH* **1993**, *23*, 31.

(8) Linder, E.; Kemmler, M.; Mayer, H. A.; Wegner, P. *J. Am. Chem. Soc.* **1994**, *116*, 348.

(9) Ramsay, J. D. F. *Pure Appl. Chem.* **1989**, *61*, 1963.

(10) Schubert, U.; Hüsing, N.; Lorenz, A. *Chem. Mater.* **1995**, *7*, 2010, and references therein.

(11) Galliot, C.; Larré, C.; Caminade, A.-M.; Majoral, J.-P. *Science* **1997**, *277*, 1981. Loup, C.; Zanta, M. A.; Caminade, A.-M.; Majoral, J.-P; Meunier, B. *Chem. Eur. J.* **1999**, *5*, 3644. Boggiano, M. K.; Soler-Illia, G. J.; Rozes, L.; Sanchez, C.; Turrin, C. O.; Caminade, A.-M.; Majoral, J.-P. *Angew. Chem., Int. Ed.*, in press.

(12) Majerle, R. S.; Bambenek, C. M.; Rice, J. A. *Polym. Prepr. (Am. Chem. Soc., Div. Polym. Chem.)* **1997**, *38*, 690.

10.1021/cm000502b CCC: $19.00 © 2000 American Chemical Society
Published on Web 12/01/2000

dendrimers on the surface of silica.[14] The hydrolysis of trialkoxysilyl-terminated dendrimers[15,16] has also been previously described under different experimental conditions, giving rise to dendrimer-based gels with various textures depending on the experimental conditions. In contrast, to the best of our knowledge, the cohydrolysis and polycondensation of dendrons bearing a hydrolyzable $Si(OEt)_3$ group at the core with an adequate number of equivalents of tetraethoxysilane (TEOS) has not been reported. This approach that we propose to develop should generate a new class of hybrid materials in which the peripheral functional groups should be accessible, allowing thus their use for different applications. Immobilization of phosphorus-containing dendrimers by this route is of particular interest as it was shown that they can present a large number of various peripheral functionalities.[17,18] In this paper, we wish to report the synthesis and the characterization of phosphorus-containing dendrimers of first, second, and third generation with various peripheral functional groups and bearing a hydrolyzable $Si(OEt)_3$ group at the core. The cohydrolysis and polycondensation of such macromolecules with a defined and variable number of equivalents of TEOS via a sol−gel protocol were studied and we report the characterization of the corresponding hybrid materials.

Experimental Section

General. All manipulations were carried out with standard high-vacuum and dry-argon techniques. ^1H, ^{13}C, and ^{31}P NMR spectra were recorded with Bruker AC 200, AC 250, or AMX 400 spectrometers. References for NMR chemical shifts are 85% H_3PO_4 for ^{31}P NMR and $SiMe_4$ for ^1H and ^{13}C NMR. The attribution of ^{13}C NMR signals has been done using J_{mod}, two-dimensional HMBC, and HMQC, Broad Band or CW ^{31}P decoupling experiments when necessary. The numbering scheme used for NMR is depicted in a figure that is reported in in the Supporting Information. Compounds **1**,[19] **3**,[20] $(EtO)_3Si(CH_2)_3PPh_2$, HOC_6H_4-*p*-PPh_2,[21] and dendrons $\mathbf{G_1'(Cl)_4}$, $\mathbf{G_2'(CN)_8}$, $\mathbf{G_2'(NMe_2)_8}$, $\mathbf{G_3'(CN)_{16}}$, and $\mathbf{G_3'(NMe_2)_{16}}$[22] were prepared according to published procedures. Some selected syntheses are described below and all the physical data concerning the others are reported in the Supporting Information.

Synthesis of the Azide 2. To a solution of azide **1** (350 mg, 1.00 mmol) in CH_2Cl_2 (25 mL) kept at 0 °C and containing activated molecular sieves (4 Å) was added under stirring a freshly prepared solution of dichlorothiophosphorhydrazide (2.05 mmol) in $CHCl_3$ (concentration 0.3 M). The reaction mixture was allowed to reach room temperature in 4 h and then filtered on Celite. The crude material was evaporated to dryness and washed twice with a mixture of pentane/ether (5/1) to afford the azide **2** as a foamy white powder in 91% yield.

$^{31}P\{^1H\}$ NMR ($CDCl_3$): δ 59.1 (s, P_0), 63.2 (s, P_1). ^1H NMR ($CDCl_3$): δ 3.30 (d, $^3J_{HP1}$ = 14.2 Hz, 6H, CH_3-N-P_1), 7.52−8.04 (m, 10H, CH=N, H_{arom}). $^{13}C\{^1H\}$ NMR ($CDCl_3$): δ 31.8 (d, $^3J_{CP1}$ = 13.4 Hz, P_1-N-CH_3), 121.8 (d, $^3J_{CP0}$ = 4.1 Hz, C_0^2), 129.0 (s, C_0^3), 131.1 (s, C_0^4), 140.2 (d, $^3J_{CP1}$ = 18.9 Hz, CH=N−N−P_1), 151.0 (d, $^2J_{CP0}$ = 8.1 Hz, C_0^1). IR (KBr): 2160 cm^{-1} (ν_{N3}). Anal. Calcd for $C_{16}H_{16}Cl_4N_7O_2P_3S_3$ (669.28): C, 28.70; H, 2.41; N, 14.65. Found: C, 28.73; H, 2.44; N, 14.62.

Synthesis of Si−$\mathbf{G_0(CHO)_2}$. To a solution of $(EtO)_3Si(CH_2)_3PPh_2$ (390 mg, 1.00 mmol) kept at 0 °C in CH_2Cl_2 (20 mL) was added dropwise a solution of azide **1** (350 mg, 1.00 mmol) in CH_2Cl_2 (20 mL). The reaction mixture was allowed to reach room temperature in 1 h and was then evaporated to dryness. The foamy crude material was washed with 20 mL of pentane/ether (2/1) to afford **Si−$\mathbf{G_0(CHO)_2}$** as a colorless thick oil in 96% yield.

$^{31}P\{^1H\}$ NMR (CD_3COCD_3): δ 20.1 (d, $^2J_{P0P'0}$ = 33.0 Hz, P_0'), 50.5 (d, $^2J_{P0P'0}$ = 33.0 Hz, P_0). ^1H NMR (CD_3COCD_3): δ 0.87 (t, $^3J_{HH}$ = 8.2 Hz, 2H, CH_2-Si), 1.22 (t, $^3J_{HH}$ = 7.0 Hz, 9H, CH_3-CH_2-O-Si), 1.86 (m, 2H, CH_2-CH_2-Si), 3.08 (td, $^3J_{HH}$ = 8.2 Hz, $^2J_{HP'0}$ = 11.0 Hz, 2H, $P_0'-CH_2$), 3.86 (q, $^3J_{HH}$ = 7.0 Hz, 6H, CH_3-CH_2-O-Si), 7.52−8.04 (m, 18H, H_{arom}), 10.11 (s, 2H, CHO). $^{13}C\{^1H\}$ NMR (CD_3COCD_3): δ 11.8 (d, $^2J_{CP'0}$ = 15.0 Hz, $P_0'-CH_2-CH_2-CH_2$), 15.9 (d, $^3J_{CP'0}$ = 3.0 Hz, $P_0'-CH_2-CH_2$), 18.0 (s, $Si-O-CH_2-CH_3$), 29.2 (d, $^1J_{CP'0}$ = 63.4 Hz, $P_0'-CH_2$), 58.2 (s, $Si-O-CH_2-CH_3$), 122.2 (d, $^3J_{CP0}$ = 5.7 Hz, C_0^2), 129.1 (d, $^2J_{CP'0}$ = 13.7 Hz, C_0^m), 129.5 (dd, $^1J_{CP'0}$ = 102.9 Hz, $^3J_{CP0}$ = 8.5 Hz, C_0^i), 131.1 (s, C_0^3), 131.6 (d, $^3J_{CP'0}$ = 11.5 Hz, C_0^o), 132.7 (br s, C_0^p), 133.3 (s, C_0^4), 157.2 (d, $^2J_{CP0}$ = 9.7 Hz, C_0^1), 191.0 (s, CHO). IR (KBr): 1702 cm^{-1} (ν_{CHO}). Anal. Calcd for $C_{35}H_{41}NO_7P_2SSi$ (709.81): C, 59.22; H, 5.82; N, 1.97. Found: C, 59.09; H, 5.71; N, 2.04.

Synthesis of Si−$\mathbf{G_1(Cl)_4}$. To a solution of $(EtO)_3Si(CH_2)_3PPh_2$ (390 mg, 1.00 mmol) kept at 0 °C in CH_2Cl_2 (20 mL) was added dropwise a solution of azide **2** (670 mg, 1.00 mmol) in CH_2Cl_2 (20 mL). The reaction mixture was allowed to reach room temperature in 1 h and was then evaporated to dryness. The foamy crude material was washed with 20 mL of a mixture of pentane/ether (2/1) to afford **Si−$\mathbf{G_1(Cl)_4}$** as a white powder in 98% yield.

$^{31}P\{^1H\}$ NMR ($CDCl_3$): δ 19.5 (d, $^2J_{P0P'0}$ = 32.8 Hz, P_0'), 51.7 (d, $^2J_{P0P'0}$ = 32.8 Hz, P_0), 63.1 (s, P_1). ^1H NMR ($CDCl_3$): δ 0.73 (t, $^3J_{HH}$ = 8.2 Hz, 2H, CH_2-Si), 1.11 (t, $^3J_{HH}$ = 7.0 Hz, 9H, CH_3-CH_2-O-Si), 1.73 (m, 2H, CH_2-CH_2-Si), 2.79 (td, $^3J_{HH}$ = 8.2 Hz, $^2J_{HP'0}$ = 11.0 Hz, 2H, $P_0'-CH_2$), 3.31 (d, $^3J_{HP1}$ = 14.1 Hz, 6H, CH_3-N-P_1), 3.71 (q, $^3J_{HH}$ = 7.0 Hz, 6H, CH_3-CH_2-O-Si), 7.12−8.04 (m, 20H, CH=N, H_{arom}). $^{13}C\{^1H\}$ NMR ($CDCl_3$): δ 11.6 (d, $^2J_{CP'0}$ = 15.0 Hz, $P_0'-CH_2-CH_2-CH_2$), 15.7 (br s, $P_0'-CH_2-CH_2$), 18.2 (s, $Si-O-CH_2-CH_3$), 29.1 (d, $^1J_{CP'0}$ = 64.2 Hz, $P_0'-CH_2$), 31.8 (d, $^3J_{CP1}$ = 13.7 Hz, CH_3-N-P_1), 58.4 (s, $Si-O-CH_2-CH_3$), 122.0 (d, $^3J_{CP0}$ = 4.1 Hz, C_0^2), 128.4 (s, C_0^3), 128.7 (d, $^2J_{CP'0}$ = 12.2 Hz, C_0^m), 129.3 (dd, $^1J_{CP'0}$ = 104.1 Hz, $^3J_{CP0}$ = 5.5 Hz, C_0^i), 130.1 (s, C_0^4), 131.5 (d, $^3J_{CP'0}$ = 10.3 Hz, C_0^o), 132.3 (d, $^4J_{CP'0}$ = 3.1 Hz, C_0^p), 141.3 (d, $^3J_{CP0}$ = 19.0 Hz, CH=N−N−P_1), 153.2 (d, $^2J_{CP0}$ = 9.3 Hz, C_0^1). Anal. Calcd for $C_{37}H_{47}Cl_4N_5O_5P_4S_3Si$ (1031.79): C, 43.07; H, 4.59; N, 6.78. Found: C, 43.17; H, 4.64; N, 6.68.

Synthesis of $\mathbf{G_1'(PPh_2)_2}$. A solution of $HOC_6H_4PPh_2$ (390 mg, 1.40 mmol) in THF (20 mL) was added to sodium hydride (33 mg, 1.40 mmol). The resulting suspension was stirred for 1 h at room temperature and then 240 mg (0.28 mmol) of $\mathbf{G_1'(Cl)_4}$ was added. The resulting mixture was stirred overnight at room temperature, then centrifuged, and evaporated to dryness. The resulting powder was washed three times with THF/pentane (1/5) to afford $\mathbf{G_1'(PPh_2)_2}$ as a white powder in 92% yield.

$^{31}P\{^1H\}$ NMR ($CDCl_3$): δ −6.3 (s, P'_2), 11.6 (d, $^2J_{PP}$ = 30.3 Hz, P_0'), 52.9 (d, $^2J_{PP}$ = 30.3 Hz, P_0), 61.9 (s, P_1). ^1H NMR ($CDCl_3$): δ 3.3 (d, $^2J_{CP}$ = 10.7 Hz, 6H, CH_3-N-P_1), 6.1−6.5 (m, 2H, CH_2=), 6.6−6.9 (m, 1H, CH=), 7.2−7.6 (m, 76H, CH=N, H_{arom}). $^{13}C\{^1H\}$ NMR ($CDCl_3$): δ 32.8 (d, $^2J_{CP}$ = 13.1 Hz, P_1-N-CH_3), 121.3 (d, $^3J_{CP}$ = 5.3 Hz, C_1^2), 121.8 (d, $^3J_{CP}$ = 4.8

(13) Chrisstoffels, L. A. J.; Adronov, A.; Fréchet, J. M. J. *Angew. Chem., Int. Ed.* **2000**, *39*, 2163.
(14) Bourque, C. S.; Maltais, F.; Xiao, W. J.; Tardif, O.; Alper, H.; Arya, P.; Manzer, L. E. *J. Am. Chem. Soc.* **1999**, *121*, 3035. Bourque, C. S.; Alper, H.; Manzer, L. E.; Arya, P. *J. Am. Chem. Soc.* **2000**, *122*, 956.
(15) Boury, B.; Corriu, R. J. P.; Nunez, R. *Chem. Mater.* **1998**, *10*, 1795.
(16) Kriesel, J. W.; Don Tilley, T. *Chem. Mater.* **1999**, *11*, 1190. Kriesel, J. W.; Don Tilley, T. *Chem. Mater.* **2000**, *12*, 1171.
(17) Launay, N.; Caminade, A.-M.; Lahana, R.; Majoral, J.-P. *Angew. Chem., Int. Ed. Engl.* **1994**, *33*, 1589. Slany, M.; Bardaji, M.; Casanove, M.-J.; Caminade, A.-M.; Majoral, J.-P.; Chaudret, B. *J. Am. Chem. Soc.* **1995**, *117*, 9764.
(18) Lartigue, M.-L.; Fayet, J.-P.; Donnadieu, B.; Galliot, C.; Caminade, A.-M.; Majoral, J.-P. *Macromolecules* **1997**, *30*, 7335.
(19) Mitjaville, J.; Caminade, A.-M.; Mathieu, R.; Majoral, J.-P. *J. Am. Chem. Soc.* **1994**, *116*, 5007.
(20) Brauge, L.; Caminade, A.-M.; Majoral, J.-P.; Wolszczak, M.; Slomkowski, S., to be published.
(21) Herd, O.; Hessler, A.; Hingst, M.; Tepper, M.; Stelzer, O. *J. Organomet. Chem.* **1996**, *522*, 69.
(22) Maraval, V.; Laurent, R.; Donnadieu, B.; Mauzac, M.; Caminade, A.-M.; Majoral, J.-P. *J. Am. Chem. Soc.* **2000**, *122*, 2499.

Scheme 1

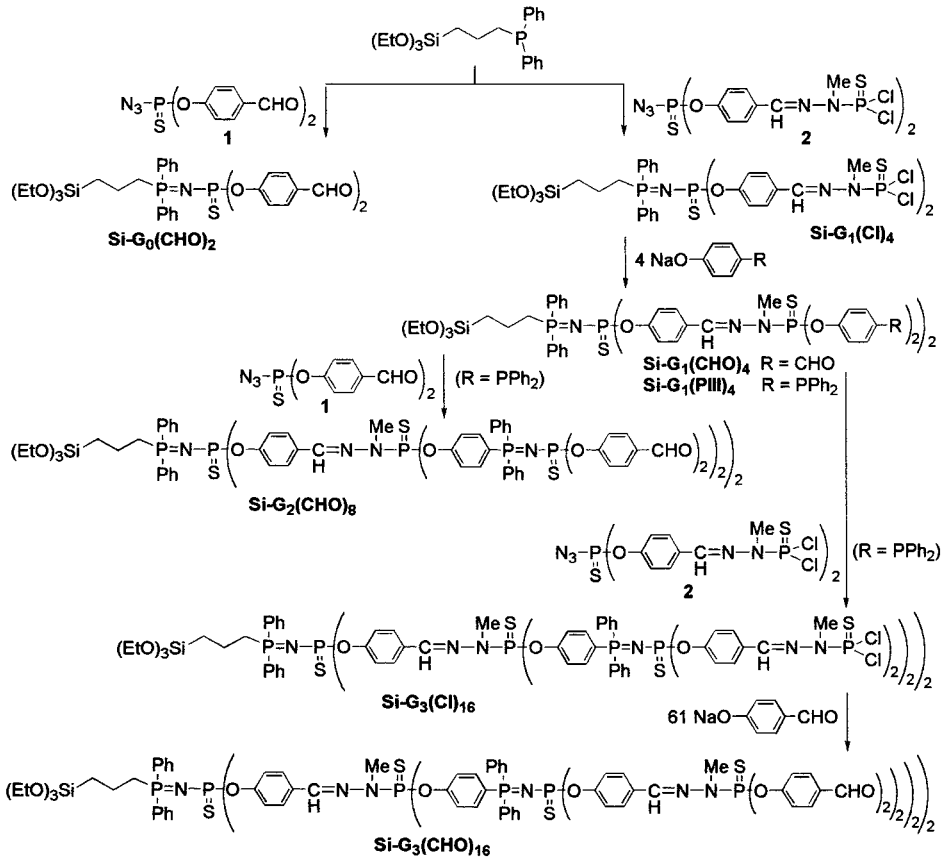

Hz, C_0^2), 127.8 (s, C_0^3), 128.4 (d, $^2J_{CP}$ = 6.9 Hz, C_2^m), 128,5 (d, $^3J_{CP}$ = 12.6 Hz, C_0^m), 128.7 (s, C_2^p), 130.7 (s, C_0^4), 132.0 (d, $^2J_{CP}$ = 10.8 Hz, C_0^o), 132.5 (s, C_0^p), 133.4 (d, $^2J_{CP}$ = 19.9 Hz, C_2^o), 133.9 (d, $^1J_{CP}$ = 11.0 Hz, C_1^4), 134.8 (d, $^2J_{CP}$ = 20.4 Hz, C_1^3), 136.6 (s, CH_2=), 136.8 (d, $^1J_{CP}$ = 11.7 Hz, C_2^i), 139.2 (d, $^3J_{CP}$ = 13.6 Hz, CH=N), 151.0 (d, $^2J_{CP}$ = 7.2 Hz, C_1^1), 152.9 (d, $^2J_{CP}$ = 8.8 Hz, C_0^1). Anal. Calcd for $C_{102}H_{85}N_5O_6P_8S_3$ (1820.80): C, 67.28; H, 4.70; N, 3.84. Found: C, 67.19; H, 4.64; N, 3.78.

Synthesis of $G_2'(Py)_8$. A solution of the pyrene azide **3** (200 mg, 0.219 mmol) in THF (10 mL) was added to a solution of dendron $G_1'(PPh_2)_4$ (100 mg, 0.055 mmol) in THF (10 mL). The resulting solution was stirred overnight at room temperature and then evaporated to dryness. The residue was washed with THF/pentane (1/5) to afford $G_2'(Py)_8$ as a beige powder in 98% yield.

$^{31}P\{^1H\}$ NMR (THF): δ 16.1 (d, $^2J_{PP}$ = 32.0 Hz, P_0'), 18.1 (d, $^2J_{PP}$ = 31.0 Hz, P_2'), 57.3 (d, $^2J_{PP}$ = 31.0 Hz, P_0, P_2), 66.5 (s, P_1). ^1H NMR (THF−d_8): δ 2.3 (m, 16H, C(O)−CH_2−CH_2), 2.9 (m, 16H, C(O)−CH_2−CH_2−CH_2), 3.4 (m, 22H, C(O)−CH_2, CH_3−N−P_1), 6.1 (ddd, $^3J_{HP}$ = 24.0 Hz, $^3J_{HHa}$ = 18.0 Hz, $^2J_{HH}$ = 1.1 Hz, 1H, Hc), 6.4 (ddd, $^3J_{HP}$ = 46.0 Hz, $^3J_{HHa}$ = 12.5 Hz, $^2J_{HH}$ = 1.1 Hz, 1H, Hb), 6.8 (dddd, $^2J_{HP}$ = 25.0 Hz, $^3J_{HHc}$ = 18.0 Hz, $^3J_{HHb}$ = 12.5 Hz, $^4J_{HP}$ = 1.1 Hz, 1H, Ha), 7.2−8.5 (m, 188H, CH=N, H_{arom}). $^{13}C\{^1H\}$ NMR (THF−d_8): δ 28.4 (s, C(O)−CH_2−CH_2), 33.7 (s, C(O)−CH_2−CH_2−CH_2), 34.2 (br s, CH_3−N−P_1), 34.6 (s, C(O)−CH_2), 122.9 (s, C_0^2, C_1^2), 123.4 (s, C_2^2), 125.2 (s, C_{py}^{13}), 126.2 (s, C_{py}^3, C_{py}^8, C_{py}^{10}), 126.5 (s, C_{py}^{15}, C_{py}^{16}), 127.2 (s, C_{py}^9), 127.9 (s, C_{py}^5), 128.6 (s, C_0^3, C_2^3, C_{py}^{12}), 129.1 (s, C_{py}^2, C_{py}^6), 130.1 (d, $^3J_{CP}$ = 12.9 Hz, C_0^m, C_2^m), 130.2 (s, C_0^4, C_{py}^{14}), 131.5 (s, C_{py}^7), 132.3 (s, C_2^4), 132.6 (s, C_{py}^{11}), 133.0 (s, C_{py}^4, C_0^p, C_2^p), 133.6 (d, $^2J_{CP}$ = 10.6 Hz, C_0^o, C_2^o), 134.0 (d, $^2J_{CP}$ = 9.3 Hz, C_1^3), 136.5 (s, CH_2=), 138.3 (s, C_{py}^1), 141.5 (br s, CH=N−N−P_1), 143.0 (s, C_2^4−CH=N), 155.0 (d, $^2J_{CP}$ = 8.5 Hz, C_1^1, C_2^1), 155.7 (br s, C_0^1), 175.7 (s, C=O). Anal. Calcd for $C_{318}H_{253}N_{25}O_{22}P_{12}S_7$ (5372.8): C, 71.09; H, 4.74; N, 6.51. Found: C, 70.95; H, 4.68; N, 6.48.

General Procedure for the Reaction of $H_2NCH_2CH_2$-$CH_2Si(OEt)_3$ with Dendrons. To a solution of dendron G_1'-$(PPh_2)_4$, $G_2'(Py)_8$, $G_2'(CN)_8$, $G_2'(NMe_2)_8$, $G_3'(CN)_{16}$, or G_3'-$(NMe_2)_{16}$ (250 mg) in THF (10 mL) was added $H_2NCH_2CH_2$-$CH_2Si(OEt)_3$ (100 equiv). The resulting solution was stirred overnight at room temperature and then evaporated to dryness. The resulting powder was washed with THF/pentane (1/5).

General Procedure for the Synthesis of Gels. To a solution of dendron (200 mg) in THF (2 mL) were added n equiv of $Si(OEt)_4$, then 3n equiv of H_2O, and then 0.01n equiv of TBAF. The resulting mixture was strongly hand-shaked. A gel progressively appeared and was allowed to age for 5 days at the gelation temperature. It was then powdered, washed with methanol, acetone, and diethyl ether, and finally dried under vacuum for 2 h at 120 °C.

Results and Discussion

Synthesis of Silylated Dendrimers. Two synthetic routes can be envisaged for the preparation of dendrons bearing a hydrolyzable $Si(OEt)_3$ group at the core and various peripheral functional groups: either the $Si(OEt)_3$ group is an intrinsic part of the dendron from the start or the $Si(OEt)_3$ group is grafted to the core after the construction of the dendron, that is, in the last step. We used both methods, which gave rise to two different lengths for the linker between the $Si(OEt)_3$ group and the dendron, this parameter being of possible importance for the gel properties.

We prepared dendrons of first, second, and third generation with aldehydes as peripheral functional groups by using the first method. The dendrons of this series will be named as follows: $Si{-}G_g$ (terminal groups)$_n$, Si to denote the presence of $Si(OEt)_3$ at the core, g, the generation number, and n, the number of end groups ($n = 2 \times 2^g$). This method consisted (Scheme 1) of reacting $(EtO)_3Si(CH_2)_3PPh_2$ with an azide according to

Scheme 2

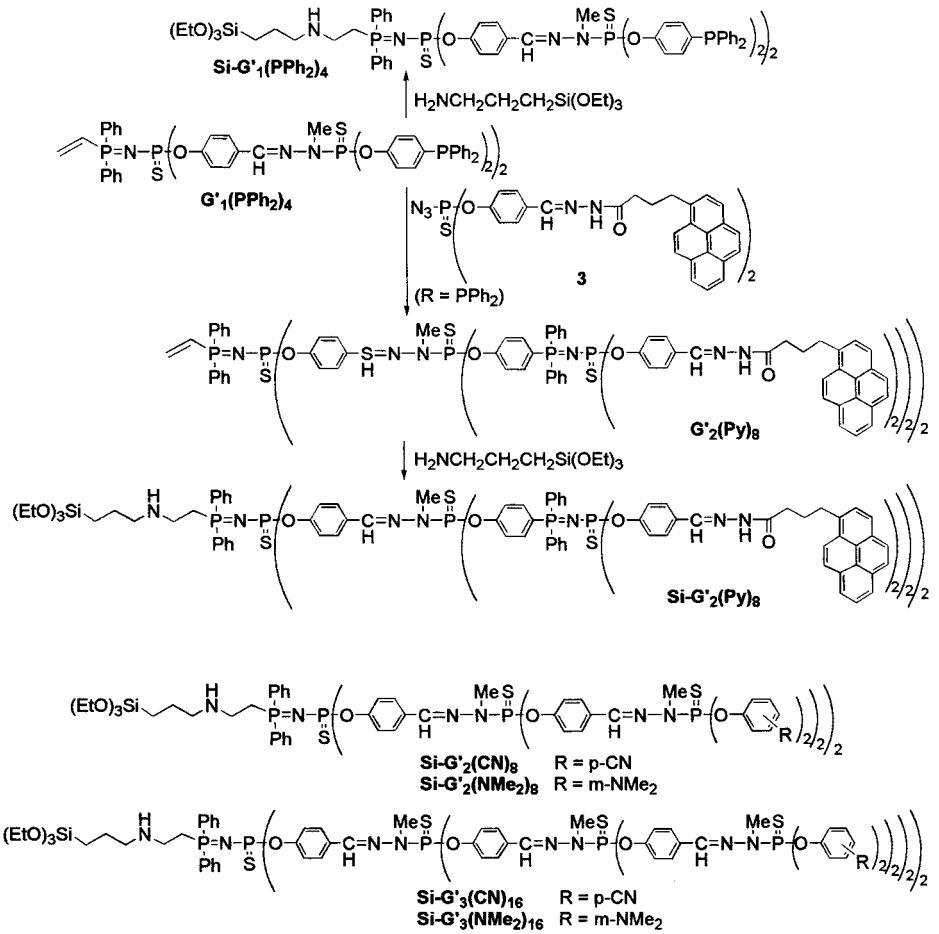

the Staudinger reaction.[23] The reaction with the azide **1**[19] afforded quantitatively compound **Si−G$_0$(CHO)$_2$**, whereas the reaction with the azide **2** led to compound **Si−G$_1$(Cl)$_4$**. In both cases, the formation of the P═N−P═S linkage was easily characterized by ^{31}P NMR spectroscopy with the appearance of two doublets at δ of ≈20 ppm (P═N) and ≈51 ppm (P═S) with $^2J_{PP}$ of ≈33 Hz. In addition to these signals, the ^{31}P NMR spectrum of **Si−G$_1$(Cl)$_4$** displayed one singlet at δ = 63.1 ppm, corresponding to the P(S)Cl$_2$ groups. The presence of CHO or P(S)Cl$_2$ groups should allow the continued growth of the dendrons in both cases. However, **Si−G$_0$(CHO)$_2$** was not used further to continue the construction of the dendrimers. Indeed, use of this product required the condensation of CHO groups with hydrazine derivatives,[17] generating water that could hydrolyze the Si(OEt)$_3$ groups prematurely. Thus, **Si−G$_0$(CHO)$_2$** was only used as a starting precursor for gel formation, and we focused our work on growing the dendrons by using the reactivity of the P(S)Cl$_2$ groups of **Si−G$_1$(Cl)$_4$** with functionalized derivatives of phenol.

The reaction of **Si−G$_1$(Cl)$_4$** with the sodium salt of 4-hydroxybenzaldehyde led to **Si−G$_1$(CHO)$_4$**, whereas **Si−G$_1$(PIII)$_4$** was obtained by reaction with the sodium salt of 4-hydroxyphenyldiphenylphosphine. Both dendrimers were characterized from their ^{31}P NMR spectra in which the signal corresponding to the phosphorus atoms that underwent the reaction (P1) were slightly shifted upfield from 63.1 ppm for Si−G$_1$(Cl)$_4$ to 60.8 for Si−G$_1$(CHO)$_4$ or 61.2 for Si−G$_1$(PIII)$_4$. Here again, dendron **Si−G$_1$(CHO)$_4$** was taken as the final product, whereas dendron **Si−G$_1$(PIII)$_4$** was used further for growing the macromolecule via the Staudinger reaction. Reaction of **Si−G$_1$(PIII)$_4$** with the azide **1** led to **Si−G$_2$(CHO)$_8$** while the reaction with the azide **2** gave rise to **Si−G$_3$(Cl)$_{16}$**. Both dendrons were characterized by their ^{31}P NMR spectra, which display two doublets at δ ≈13 (P═N) and ≈50 ppm (P═S) in addition to those attributed to the P═N−P═S linkage of the core, thus indicating the formation of the new P═N−P═S linkages. Finally, reaction of **Si−G$_3$(Cl)$_{16}$** with the sodium salt of 4-hydroxybenzaldehyde yielded the dendron **Si−G$_3$(CHO)$_{16}$**. The ^{31}P NMR spectrum of this last dendron **Si−G$_3$(CHO)$_{16}$** exhibits two sets of two doublets and two singlets, the Si(OEt)$_3$ group at the core being characterized by ^{1}H and ^{13}C NMR spectroscopies. The complete series of dendrons prepared by this route was named the **A** series.

The second method consisted of synthesizing first a dendron without any hydrolyzable Si(OEt)$_3$ group and then of grafting the Si(OEt)$_3$ group at the core during the last step to afford compounds of the **B** series. These dendrons will be named G$_g$′(terminal groups)$_n$. This method avoids any risk of unwanted hydrolysis during the synthesis of the dendron. However, it requires a functional group at the core unable to react during the synthesis of the dendron but allowing the grafting of the Si(OEt)$_3$ group in the last step. We have already

(23) Staudinger, H.; Meyer, J. *Helv. Chim. Acta* **1919**, *2*, 635.

demonstrated that a vinyl group linked to a P═N−P═S group presents such properties; it can undergo Michael additions with primary or secondary amines.[22] Therefore, we used this reaction to silylate dendrons of first, second, and third generation with various pheripheral groups, all the dendrons bearing a vinyl group at the core. First, we attempted to silylate the dendron **$G_1'(PPh_2)_4$** by treating it with a large excess (100 equiv) of 3-aminopropyltriethoxysilane (Scheme 2). The addition reaction occurred easily to give compound **$Si-G_1'(PPh_2)_4$** in high yield. **$Si-G_1'(PPh_2)_4$** was characterized by ^{31}P NMR spectroscopy, the doublet corresponding to the P═N group of the P═N−P═S linkage appearing at 17.8 ppm, while for the starting compound **$G_1'(PPh_2)_4$** the signal attributed to this group was at 11.6 ppm. **$Si-G_1'(PPh_2)_4$** was further characterized by ^1H and ^{13}C NMR spectroscopies, which revealed the disappearance of the signals assigned to the vinyl group and the appearance of those corresponding to the NCH_2CH_2P linkage. It is worth noting that compounds **$Si-G_1'(PPh_2)_4$** and **$Si-G_1(PIII)_4$** differ only by the length of the linker between the $Si(OEt)_3$ group and the P═N−P═S linkage of the dendron, that is, four bonds for **$Si-G_1(PIII)_4$** and seven bonds for **$Si-G_1'(PPh_2)_4$**.

Next, we used the Staudinger reaction to grow the dendron **$G_1'(PPh_2)_4$**. However, instead of treating **$G_1'(PPh_2)_4$** with the azides **1** or **2** as previously done to obtain similar dendrons to those obtained in the **A** series, we preferred to use the fluorescent azide **3**,[20] bearing two pyrene groups to bring new properties to the dendron. The Staudinger reaction between **$G_1'(PPh_2)_4$** and **3** (Scheme 2) leads quantitatively to the dendron of second generation **$G_2'(Py)_8$**, the ^{31}P NMR spectrum of which exhibited two sets of two doublets, attributed to two types of P═N−P═S linkages in a 1/4 ratio as expected.

$G_2'(Py)_8$ as well as other dendrons of second and third generation, which were previously described **($G_2'(CN)_8$, $G_2'(NMe_2)_8$, $G_3'(CN)_{16}$,** and **$G_3'(NMe_2)_{16}$**[22]**)**, all of them bearing a vinyl group at the core, were successfully silylated via the Michael addition with $H_2N(CH_2)_3Si(OEt)_3$. Dendrons **$Si-G_2'(CN)_8$**, **$Si-G_2'(NMe_2)_8$**, **$Si-G_3'(CN)_{16}$**, and **$Si-G_3'(NMe_2)_{16}$** were thus isolated in nearly quantitative yields (Scheme 2). Their ^{31}P, ^1H, and ^{13}C NMR spectra displayed the expected signals for such compounds.

Thus, both methods of synthesis gave rise to dendrons having in all cases a hydrolyzable $Si(OEt)_3$ group at the core. They differ by the length of the linker between the $Si(OEt)_3$ group and the dendron (four or seven bonds), by the generation (from 0 to 3), by the number (from 2 to 16), and by the nature of the peripheral functional groups (phosphine, aldehyde, pyrene, cyano, or dimethylamino).

Sol−Gel Processing and Nomenclature. The cohydrolysis and polycondensation of silylated macromolecules were performed at room temperature in THF solution with 1 mol % of TBAF as catalyst. The number of equivalents of water was always 3 times that of TEOS, which corresponds to an excess of water. For the dendrons of the **A** series, the number of equivalents of TEOS was regularly increased until the gelation took place, as indicated in Table 1. It appears from these results that the higher the dendrimer generation, the greater the demanded quantity of TEOS for the gelation. Thus, the gelation of **$Si-G_0(CHO)_2$** required at least 10 equiv of TEOS, that of **$Si-G_1(CHO)_4$**, 20 equiv, that of **$Si-G_2(CHO)_8$** 40 equiv, while 140 equiv of TEOS was necessary for the gelation of **$Si-G_3(CHO)_{16}$**. The powders obtained after the workup given in the Experimental Section were described by the following nomenclature: first, an X to denote xerogels followed by the number *n* of equiv of TEOS used for the gelation, and then by the designation of the silylated macromolecules. As an example, the material resulting from the cogelification of **$Si-G_1(CHO)_4$** and of 50 equiv of TEOS was named **$X50Si-G_1(CHO)_4$**.

Table 1. Textural Data for the Materials Prepared by Cohydrolysis and Polycondensation of TEOS and of Dendrimers of the A Series

entry	dendrimer	n_{equiv} TEOS	BET surface area ($m^2\,g^{-1}$)	total pore volume ($cm^3\,g^{-1}$)	micropore volume[b] ($cm^3\,g^{-1}$)	density[c] (g/cm^3)
1	$Si-G_0(CHO)_2$	5[a]				
2	$Si-G_0(CHO)_2$	10	135	0.45	0	1.73
3	$Si-G_0(CHO)_2$	20	330	*d*	*d*	1.75
4	$Si-G_0(CHO)_2$	30	395	0.31	0.12	1.80
5	$Si-G_0(CHO)_2$	50	590	0.65	0.17	1.88
6	$Si-G_0(CHO)_2$	100	520	*d*	*d*	2.00
7	$Si-G_0(CHO)_2$	200	560	0.47	0.18	1.98
8	$Si-G_0(CHO)_2$	500	550	*d*	*d*	2.10
9	$Si-G_1(CHO)_4$	5[a]				
10	$Si-G_1(CHO)_4$	10[a]				
11	$Si-G_1(CHO)_4$	20	170	*d*	*d*	1.66
12	$Si-G_1(CHO)_4$	30	270	*d*	*d*	1.70
13	$Si-G_1(CHO)_4$	50	280	*d*	*d*	1.80
14	$Si-G_1(CHO)_4$	100	300	*d*	*d*	1.83
15	$Si-G_1(CHO)_4$	200	380	0.35	0.13	1.84
16	$Si-G_1(CHO)_4$	500	340			1.91
17	$Si-G_1(CHO)_4$	1000	370	0.51	0.10	1.98
18	$Si-G_1(PIII)_4$	10[a]				
19	$Si-G_1(PIII)_4$	20	10			1.60
20	$Si-G_1(PIII)_4$	30	160	*d*	*d*	1.66
21	$Si-G_1(PIII)_4$	50	420	*d*	*d*	1.76
22	$Si-G_2(CHO)_8$	5[a]				
23	$Si-G_2(CHO)_8$	10[a]				
24	$Si-G_2(CHO)_8$	20[a]				
25	$Si-G_2(CHO)_8$	30[a]				
26	$Si-G_2(CHO)_8$	40	165	*d*	*d*	1.80
27	$Si-G_2(CHO)_8$	50	195	*d*	*d*	1.79
28	$Si-G_2(CHO)_8$	60	200	*d*	*d*	1.86
29	$Si-G_2(CHO)_8$	200	330	0.32	0.10	1.87
30	$Si-G_2(CHO)_8$	500	460	*d*	*d*	1.90
31	$Si-G_2(CHO)_8$	1000	350	0.31	0.12	1.92
32	$Si-G_2(CHO)_8$	2000	360	0.36	0.12	1.95
33	$Si-G_3(CHO)_{16}$	30[a]				
34	$Si-G_3(CHO)_{16}$	40[a]				
35	$Si-G_3(CHO)_{16}$	50[a]				
36	$Si-G_3(CHO)_{16}$	60[a]				
37	$Si-G_3(CHO)_{16}$	70[a]				
38	$Si-G_3(CHO)_{16}$	140	245	0.42	0	1.84
39	$Si-G_3(CHO)_{16}$	280	185	*d*	*d*	1.86
40	$Si-G_3(CHO)_{16}$	410	320	0.45	0.1	1.85

[a] No gelation after a long reaction time. [b] Determined by the *t*-plot method. [c] At 25 °C. [d] Not determined.

Solid State ^{31}P and ^{29}Si NMR Spectroscopy. The solid state ^{31}P NMR spectroscopy provides information concerning the dendrimer moieties incorporated into silica. We have reported the solution ^{31}P NMR chemical shifts of dendrimers as well as those of the corresponding dendrimer−silica xerogels in Table 2. The solids prepared from **$Si-G_0(CHO)_2$** display two resonances as expected in the same range as those observed in solution (Table 2, entries 1−7). For the others, the number of resonances observed from solid state ^{31}P NMR spectroscopy is always inferior to that observed in solution ^{31}P NMR. Indeed, as the relative intensity of the signal

Table 2. Solution ^{31}P NMR Chemical Shifts of Dendrimer Precursors and Solid State ^{31}P NMR Chemical Shifts of Corresponding Dendrimer−Silica Xerogels

entry	dendrimer	solution ^{31}P NMR δ (ppm)	xerogel	HPDEC ^{31}P NMR δ (ppm)
1	Si−$G_0(CHO)_2$	20.1, 50.5	X10Si−$G_0(CHO)_2$	19.7, 50.7
2			X20Si−$G_0(CHO)_2$	20.5, 49.8
3			X30Si−$G_0(CHO)_2$	20.5, 50.3
4			X50Si−$G_0(CHO)_2$	21.7, 51.9
5			X100Si−$G_0(CHO)_2$	21.3, 51.0
6			X200Si−$G_0(CHO)_2$	20.8, 51.5
7			X500Si−$G_0(CHO)_2$	19.2, 52.8
8	Si−$G_1(CHO)_4$	19.9, 52.2, 60.8	X20Si−$G_1(CHO)_4$	18.3, 59.6
9			X30Si−$G_1(CHO)_4$	18.8, 59.6
10			X50Si−$G_1(CHO)_4$	19.5, 60.8
11			X100Si−$G_1(CHO)_4$	19.2, 60.0
12			X200Si−$G_1(CHO)_4$	18.6, 60.3
13			X500Si−$G_1(CHO)_4$	19.2, 59.5
14			X1000Si−$G_1(CHO)_4$	19.6, 61.2
15	Si−$G_2(CHO)_8$	13.6, 19.2, 50.0, 51.7, 60.7	X40Si−$G_2(CHO)_8$	12.6, 50.3
16			X50Si−$G_2(CHO)_8$	14.3, 49.8
17			X60Si−$G_2(CHO)_8$	13.0, 50.3
18			X200Si−$G_2(CHO)_8$	14.3, 51.0
19			X500Si−$G_2(CHO)_8$	16.5, 49.3
20			X1000Si−$G_2(CHO)_8$	13.5, 50.7
21			X2000Si−$G_2(CHO)_8$	13.5, 51.5
22	Si−$G_3(CHO)_{16}$	13.2, 19.2, 51.0, 51.8, 60.7, 61.1	X140Si−$G_3(CHO)_{16}$	11.7, 59.6
23			X280Si−$G_3(CHO)_{16}$	13.0, 60.9
24			X410Si−$G_3(CHO)_{16}$	11.7, 60.4
25	Si−$G_1(PIII)_4$	−6.5, 18.4, 51.5, 61.2	X20Si−$G_1(PIII)_4$	−6.4, 19.2, 62.2
26			X30Si−$G_1(PIII)_4$	−6.0, 21.4, 63.3
27			X50Si−$G_1(PIII)_4$	−6.5, 18.0, 62.7
28	Si−$G'_1(PPh_2)_4$	−6.3, 17.8, 52.3, 62.0	X30Si−$G'_1(PPh_2)_4$	−6.5, 17.5, 62.7
29	Si−$G'_2(Py)_8$	11.9, 17.4, 51.1, 60.4	X80Si−$G'_2(Py)_8$	13.5, 52.0
30	Si−$G'_2(CN)_8$	18.0, 52.4, 60.2, 61.9	X40Si−$G'_2(CN)_8$	17.5, 60.9
31			X80Si−$G'_2(CN)_8$	16.6, 62.7
32	Si−$G'_2(NMe_2)_8$	17.5, 51.8, 61.8	X20Si−$G'_2(NMe_2)_8$	17.9, 63.6
33			X30Si−$G'_2(NMe_2)_8$	17.9, 63.1
34			X40Si−$G'_2(NMe_2)_8$	17.9, 63.1
35			X80Si−$G'_2(NMe_2)_8$	16.6, 64.9
36	Si−$G'_3(CN)_{16}$	18.0, 52.0, 60.3, 61.6	X80Si−$G'_3(CN)_{16}$	17.0, 60.5
37	Si−$G'_3(NMe_2)_{16}$	17.9, 52.2, 62.5, 62.8	X70Si−$G'_3(NMe_2)_{16}$	17.9, 63.6
38			X80Si−$G'_3(NMe_2)_{16}$	17.0, 63.1

corresponding to phosphorus centers located at the periphery is always superior to others, this signal screens that of the phosphorus centers in close proximity. This is illustrated in Figure 1, which reported the solid state ^{31}P NMR spectra of **X20Si−$G_0(CHO)_2$**, **X20Si−$G_1(CHO)_4$**, **X40Si−$G_2(CHO)_8$**, and **X140Si−$G_3(CHO)_{16}$**.

From these data, it can be concluded that the dendrimers were not damaged during the sol−gel process.

The solid state ^{29}Si NMR spectra of some dendrimer−silica xerogels have been recorded. That of **X20Si−$G_0(CHO)_2$** was given as an example in Figure 2. It exhibits a weak signal at −91.4 ppm, a large one at −100.9 ppm, and a weak one at −109.7 ppm, respectively assigned to the Q^2 $(SiO)_2Si(OR)_2$, Q^3 $(SiO)_3SiOR$, and Q^4 $(SiO)_4Si$ sites of the framework. Furthermore, it displays poor resonances at −58.5 and −65.0 ppm, attributed to T^2 [C−Si(OR)$(OSi)_2$] and T^3 [C−Si$(OSi)_3$] sites. As the ^{29}Si NMR spectrum of **Si−$G_0(CHO)_2$** displayed a signal at −46.5 ppm in $CDCl_3$, it can be concluded that the dendrimers are not simply encapsulated[24] within the silica but covalently linked to the silica matrix by one Si−C bond.

Nitrogen Adsorption Measurements. First, it is to be noted, that under the experimental conditions used for the preparation of dendrimer−silica xerogels, hydrolysis and polycondensation of TEOS gives rise to an essentially microporous silica with a specific surface area of 600 m^2 g^{-1}. Nitrogen BET measurements gave specific surface areas that depend on the nature of the dendrimer. Indeed, the surface areas of materials prepared from the **A** series of dendrimers (Table 1) lie between 10 m^2 g^{-1} (entry 19) and 590 m^2 g^{-1} (entry 5), depending on the "dilution" of the macromolecules in the silica. It clearly appears that for a generation number there is an increase in the BET surface areas of materials with the amount of TEOS used to get a gel. For a given number "*n*" of equivalents of TEOS, the surface area decreases as the generation number increases (for example, compare entries 5, 13, and 27). A likely explanation for this phenomenon could be that the gel precursor **Si−$G_3(CHO)_{16}$** exhibits a degree of compressibility superior to that of generation 2 and that of generation 2 more than that of generation 1. However, this effect is attenuated as the dilution increases (for example, compare entries 7, 15, and 29). All the xerogels prepared from dendrimers of the **A** series exhibited isotherms intermediate between type I (characteristic of microporous solids) and II (characteristic of nonporous solids or with large pores) according to the BDDT classification.[25] A representative N_2 adsoption−desorption isotherm for these materials is displayed in

(24) Chujo, Y.; Matsuki, H.; Kure, S.; Saegusa, T.; Yazawa, T. *Chem. Commun*. **1994**, 635. Huang, J.; Sooklal, K.; Murphy, C. J.; Ploehn, H. J. *Chem. Mater*. **1999**, *11*, 3595. Larsen, G.; Lotero, E.; Marquez, M. *J. Phys. Chem. B* **2000**, *104*, 4840. Larsen, G.; Lotero, E.; Marquez, M. *Chem. Mater*. **2000**, *12*, 1513.

(25) Brunauer, S.; Deming, L. S.; Deming, W. E.; Teller, E. *J. Am. Chem. Soc*. **1940**, *62*, 1723

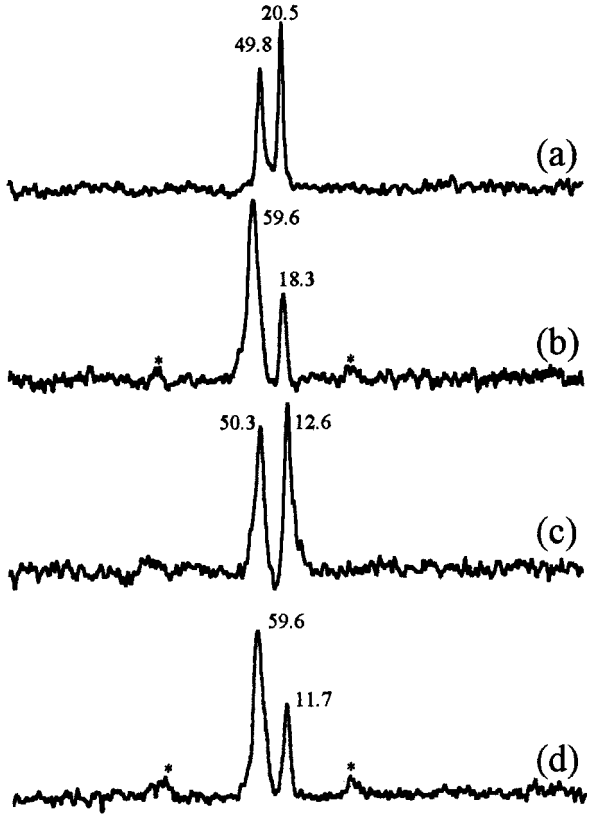

Figure 1. Solid state ^{31}P HPDEC NMR spectra of (a) X20Si−$G_0(CHO)_2$, (b) X20Si−$G_1(CHO)_4$, (c) X40Si−$G_2(CHO)_8$, and (d) X140Si−$G_3(CHO)_8$. ^{31}P NMR experiments were performed on a Bruker ASX 2000 spectrometer at a ^{31}P frequency of 81.0 MHz at room temperature. Chemical shifts were referenced to K_2HPO_4 at 0 ppm. Signals arising from sidebands are marked with asterisks.

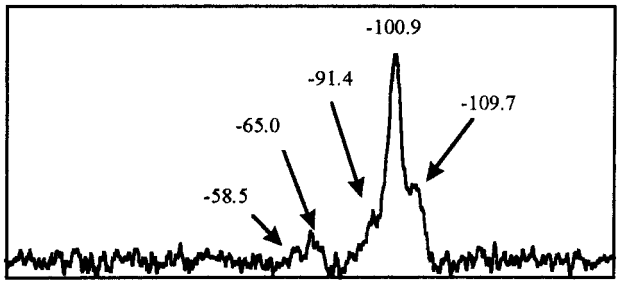

Figure 2. Solid state ^{29}Si CP MAS NMR spectrum of X20Si−$G_0(CHO)_2$. ^{29}Si NMR experiment was performed on a Bruker ASX 200 spectrometer at a ^{29}Si frequency of 39.7 MHz at room temperature. Chemical shifts were referenced to TMS at 0 ppm.

Figure 3. Analysis of data by the *t*-plots method[26] revealed in most samples a broad pore size distribution (see the insert in Figure 3) with the presence of micropores as well as meso- and macropores with pore diameters lying from 50 to 1000 Å according to the BJH method. It is interesting to compare the texture of the material **X30Si−G$_1$(PIII)$_4$** (**A** series, entry 20, Table 1) with that of **X30Si−G$_1$′(PPh$_2$)$_4$** (**B** series, entry 2, Table 3). Indeed, the only difference between the precursors of these materials comes from the linker between the silicon atom and the dendron moiety, linker which is of

(26) Gregg, S. J.; Sing, K. S. W. *Adsorption, Surface Area and Porosity*, 2nd ed.; Academic Press: New York, 1982.

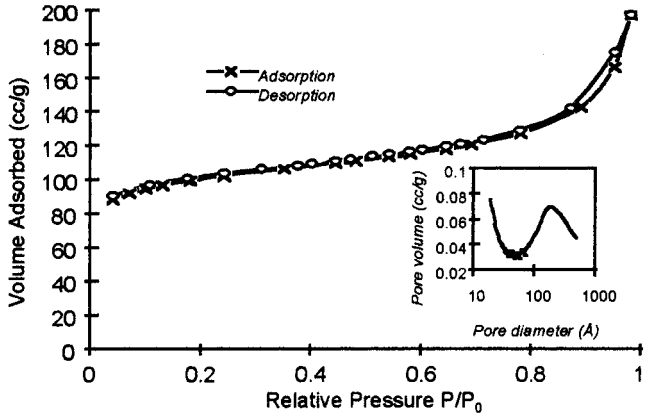

Figure 3. N_2 adsorption−desorption isotherms for X1000Si−$G_2(CHO)_g$ at 77 K. The insert shows the BJH pore size distribution calculated from the desorption branch of the isotherm.

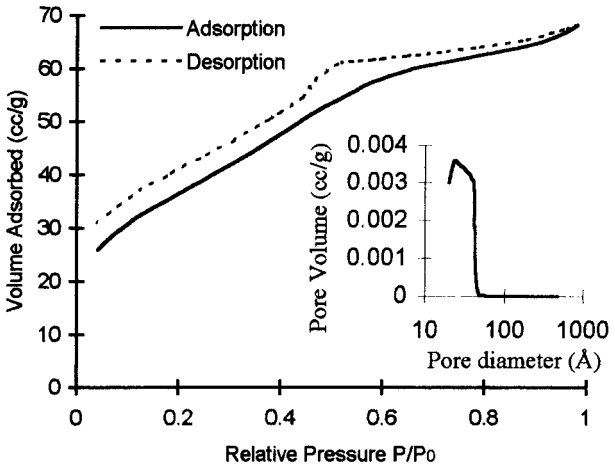

Figure 4. N_2 adsorption−desorption isotherms for X80Si−$G_2'(Py)_g$ at 77 K.

3C for **Si−G$_1$(PIII)$_4$** and of 5C and 1N for **Si−G$_1$′-(PPh$_2$)$_4$**. **X30Si−G$_1$(PIII)$_4$** is mesoporous with a broad pore size distribution while **X30Si−G$_1$′(PPh$_2$)$_4$** is nonporous. That clearly indicates that the length of the linker is of importance for the texture of the material. Furthermore, the materials of the **B** series present textural data that are different from those of the **A** series. Some materials (Table 3) are nonporous (entries 2, 6, 9, 10, and 11) and others are mesoporous with a large pore size distribution (entry 3, Figure 4, entries 12 and 14) or mesoporous with a narrow pore size distribution, which is worth noting (entries 7, 17, and 18, Figure 5). It is another indication of the importance of the length of the linker between silicon and the dendron moiety for the texture of the materials, as such a texture was not obtained from precursors of the **A** series. However, it is clear that the texture should result from the conjunction of several other factors such as generation number, coefficient of dilution (n_{equiv} of TEOS), and nature of peripheral groups. The results obtained up to now permit prediction of neither the texture of the dendrimer−silica xerogels nor that of other hybrid organic materials.

Elemental and Thermal Analysis. Elemental and thermal analyses were performed to calculate the percentage of the organic part that was incorporated

Table 3. Textural Data for the Materials Prepared by Cohydrolysis and Polycondensation of TEOS and of Dendrimers of the B Series

entry	dendrimer	n_{equiv} TEOS	BET surface area ($m^2\,g^{-1}$)	pore volume ($cm^3\,g^{-1}$)	micropore volume[a] ($cm^3\,g^{-1}$)	BJH pore diameter[b] (Å)	density[c] (g/cm^3)
1	$Si-G_1'(PPh_2)_4$	20[d]					
2	$Si-G_1'(PPh_2)_4$	30	<5				1.55
3	$Si-G_2'(Py)_8$	80	132	0.11	0.02	from 20 to 50	1.61
4	$Si-G_2'(CN)_8$	20[d]					
5	$Si-G_2'(CN)_8$	30[d]					
6	$Si-G_2'(CN)_8$	40	<5				1.61
7	$Si-G_2'(CN)_8$	80	405	0.43	0	38	1.78
8	$Si-G_2'(NMe_2)_8$	10[d]					
9	$Si-G_2'(NMe_2)_8$	20	5				1.53
10	$Si-G_2'(NMe_2)_8$	30	6				1.56
11	$Si-G_2'(NMe_2)_8$	40	12				1.59
12	$Si-G_2'(NMe_2)_8$	80	360	0.78	0	from 20 to 400	1.78
13	$Si-G_3'(CN)_{16}$	70[d]					
14	$Si-G_3'(CN)_{16}$	80	175	0.59	0	from 20 to 400	1.74
15	$Si-G_3'(NMe_2)_{16}$	10[d]					
16	$Si-G_3'(NMe_2)_{16}$	20[d]					
17	$Si-G_3'(NMe_2)_{16}$	70	142	0.24	0	40	1.66
18	$Si-G_3'(NMe_2)_{16}$	80	166	0.27	0	45	1.75

[a] Determined by the *t*-plot method. [b]Determined from the maxima of BJH desorption pore size distribution curve with the Halsey equation. [c]At 25 °C. [d]No gelation after a long reaction time.

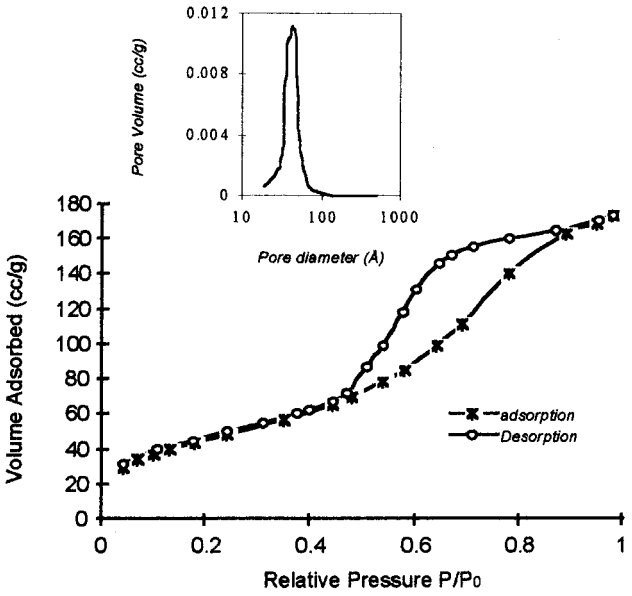

Figure 5. N_2 adsorption−desorption isotherms of $X80Si-G_3'-(NMe_2)_{16}$ at 77 K. The insert shows the BJH pore size distribution calculated from the desorption branch of the isotherm.

into the materials. We have reported in Table 4 the theoretical and found Si/P ratio from elemental analysis. The percentage of the introduced organic part was inferred from these data. It appears that this percentage is always inferior to the theoretical value. That should be due to the difference between the rate of hydrolysis and polycondensation of the silylated dendrimer and of TEOS. As the molecular weights of the precursors are much higher than those of TEOS, any amount of nonhydrolyzed precursor leads to an important loss of organic part into the hybrid material. Nevertheless, the amount of incorporated dendrimer into a silica matrix was always notable.

Thermogravimetric analyses (TGA) under air were performed from room temperature to 1200 °C. All the dendrimers−silica xerogels displayed the same general pattern; as an example, the TGA curve of

Table 4. Amount of Organic Part Incorporated into the Silica Matrix from Elemental and Thermal Analysis

		Si/P ratio		amount of org. introduced		
entry	xerogel	theor.	found[a]	% theor.	% found[a]	% found[b]
1	$X10Si-G_0(CHO)_2$	5.5	7.5	45.4	33.3	29.9
2	$X20Si-G_0(CHO)_2$	10.5	16.8	30.2	18.9	17.7
3	$X30Si-G_0(CHO)_2$	15.5	17.3	22.7	20.3	17.4
4	$X20Si-G_1(CHO)_4$	5.2	6.8	49.1	37.5	*c*
5	$X30Si-G_1(CHO)_4$	7.7	10.1	39.5	30.1	23.6
6	$X50Si-G_1(CHO)_4$	12.7	18.2	28.4	19.8	18.7
7	$X40Si-G_2(CHO)_8$	3.4	10.8	55.9	17.6	22.7
8	$X50Si-G_2(CHO)_8$	4.2	12.2	50.5	17.4	22.8
9	$X60Si-G_2(CHO)_8$	5.1	16.1	46.0	14.6	19.9
10	$X200Si-G_2(CHO)_8$	16.7	40.0	20.5	8.2	15.4
11	$X140Si-G_3(CHO)_{16}$	7.0	16.6	40.5	17.1	23.0
12	$X280Si-G_3(CHO)_{16}$	14.0	28.3	25.5	12.6	16.2
13	$X410Si-G_3(CHO)_{16}$	20.5	36.7	18.9	10.6	14.4
14	$X20Si-G_1(PIII)_4$	2.6	5.6	59.4	27.6	31.7
15	$X30Si-G_1(PIII)_4$	3.9	8.3	49.7	23.3	28.7
16	$X50Si-G_1(PIII)_4$	6.4	23.0	37.5	10.4	19.4
17	$X30Si-G_1'(PPh_2)_4$	3.9	4.8	50.3	40.8	30.8
18	$X80Si-G_2'(Py)_8$	6.7	10.3	52.8	34.3	36.8
19	$X40Si-G_2'(CN)_8$	5.1	6.0	51.0	43.3	33.3
20	$X80Si-G_2'(CN)_8$	10.1	12.1	34.5	28.8	24.7
21	$X20Si-G_2'(NMe_2)_8$	2.6	3.7	68.3	48.0	45.4
22	$X30Si-G'_2(NMe_2)_8$	3.9	5.0	59.3	46.2	39.9
23	$X40Si-G_2'(NMe_2)_8$	5.1	6.0	52.4	44.5	37.1
24	$X80Si-G_2'(NMe_2)_8$	10.1	13.9	35.8	26.0	27.6
25	$X80Si-G_3'(CN)_{16}$	5.0	13.1	51.7	19.7	25.2
26	$X70Si-G_3'(NMe_2)_{16}$	4.4	8.6	56.3	28.8	32.3
27	$X80Si-G_3'(NMe_2)_{16}$	5.0	11.6	53.0	22.8	28.0

[a] From elemental analysis. [b]By thermogravimetric analyses. [c]Not determined.

$X20Si-G_0(CHO)_2$ is presented in Figure 6: after a weight loss corresponding to the removal of water, an onset of decomposition occurred near 250 °C with complete oxidation to silica by about 700 °C. Above this temperature, almost no weight loss was observed up to the final temperature of 1200 °C. The percentages of introduced organic part inferred from the TGA curves are given in Table 4. All the data were corrected, taking into account the weight loss observed on the TGA curve of the silica prepared under the same conditions as those of the dendrimer−silica xerogels. Indeed, the TGA curve of the silica displays a weight loss of 11% between 200

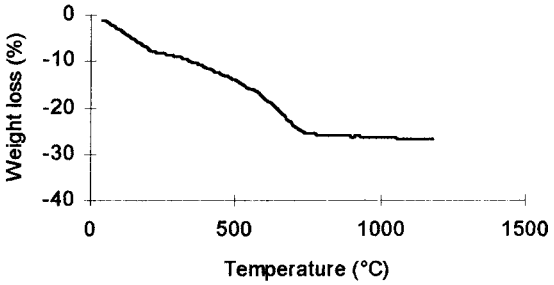

Figure 6. Thermogravimetric analysis trace (air, 10 °C/min) of $X20Si-G_0(CHO)_2$.

and 700 °C, which is due to further condensation. Thus, it appears that the percentage of organic part found from the TGA curves is always inferior to the theoretical percentage of introduced organic part as it was previously observed from the elemental analysis.

Conclusion

The preparation of dendrons bearing a hydrolyzable $Si(OEt)_3$ group at the core has been achieved by two routes: either the $Si(OEt)_3$ group was a part of the dendron from the start (**A** series) or the $Si(OEt)_3$ group was grafted to the core in the last step of the construction of the dendron (**B** series). The first method allows the preparation of dendrons with very reactive peripheral groups such as $P(S)Cl_2$ or CHO. However, the risk of unwanted hydrolysis during the synthesis of the dendron is inherent in the method and constitutes the main drawback. The second method succeeded via the Michael reaction of the 3-aminopropyltriethoxysilane with a vinyl group linked to a P═N−P═S group. The choice of the peripheral groups by this route is limited, as they should not react with the primary amino groups. However, this method allows the change of the length of the linker between the dendron and the $Si(OEt)_3$ group at the last step of the synthesis of the dendron, which is an advantage over the first method. Indeed, the study of the texture of dendrimer−silica xerogels showed that the length of the linker played a role in the gelation behavior. Furthermore, this second route avoided the risk of hydrolysis during the growth of the dendron.

Thus, we can put forward that both the methods are complementary and allow the preparation of a large variety of silylated dendrons, giving rise by cohydrolysis and polycondensation with TEOS to the corresponding dendrimer−silica xerogels. It is worth noting that dendrons with terminal phosphino groups can be achieved by both methods. Such functions are of special interest as their metal complexes can lead, after cogelification, to a new class of supported catalysts.

CM000502B